Selection of Radio Sources for Venus Balloon-Pathfinder ΔDOR Navigation at 1.7 GHz

K. M. Liewer[1]
TDA Engineering Office

In order to increase the success rate of the ΔDOR VLBI navigational support for the French-Soviet Venus Balloon and Halley Pathfinder projects, forty-four extragalactic radio sources were observed in advance of these projects to determine which were suitable for use as reference sources. Of these forty-four radio sources, taken from the existing JPL radio source catalogue, thirty-six were determined to be of sufficient strength for use in ΔDOR VLBI navigation.

I. Introduction

The technique of Very Long Baseline Interferometery (VLBI) (Refs. 1–3) is used to achieve the navigational accuracy required by many projects (Refs. 4, 5). The particular method used for navigation of the Soviet spacecraft VEGA is the ΔDOR (delta-Differential One-way Range) technique. This technique estimates the angular position of the spacecraft on the plane of the sky relative to a reference radio source. Delta-DOR uses the difference in arrival time of a spacecraft signal between two stations (equivalent to a differential one way range measurement) and differences this result with a similar measurement made on a nearby extragalactic radio source (EGRS). The differencing of the spacecraft delay and the EGRS delay results in the partial cancellation of many error sources that are common to the two measurements. This differencing also means the spacecraft position is only determined relative to that of the EGRS. As a result, the positions of the EGRS must be well known if the ΔDOR measurements are to be useful for navigation.

The degree to which the common error sources are canceled in ΔDOR measurements increases as the angular separation of the spacecraft and reference radio source decreases. It is therefore desirable to have a distribution of EGRS on the sky with sufficient density so that the angular distance between a spacecraft and one of the EGRS is 10 degrees or less. The Deep Space Network currently observes more than 130 extragalactic radio sources in order to obtain a catalogue of source positions with sufficient accuracy and coverage to meet navigational requirements. The accuracy of this catalogue is currently about 50 nanoradians (10 milliarcseconds).

The catalogue available prior to the VEGA mission was derived from observations made at 2.3 GHz (S band) and 8.4 GHz (X band) with most of the weight from the 8.4 GHz observations. The transmissions from the VEGA spacecraft, however, were at 1.7 GHz (L band). This presented two possible problems: (1) The source position at 1.7 GHz could

[1]The work described in this article was performed when the author was a member of the Tracking Systems and Applications Section.

differ from that determined from the 2.3/8.4 GHz observations; and (2) the correlated flux density, which is the strength of a source measured with VLBI, was not known at 1.7 GHz for any of the sources in the catalogue.

Because of the small amount of time available for making new observations and the lack of dual frequency observations to correct for charged particle effects, 1.7 GHz positions with errors at the 50 nanoradian level could not be produced. Inspection of the radio maps of several radio sources made near 1.7 and 8.4 GHz indicated that the positions determined using these frequencies would differ by less than 10 nanoradians for most sources (J. S. Ulvestad, private communication, 1985). The decision was therefore made to adopt the positions from the existing 2.3/8.4 GHz catalogue.

Because the transmission schedules of the Russian spacecraft were such that there were relatively few opportunities for making ΔDOR observations, it was very important that the success rate for these observations be as high as possible. To be assured that the observations did not fail due to lack of sufficient signal from the EGRS, measurements of the L band correlated flux density of potential navigation sources were necessary prior to the ΔDOR observations.

II. Description of Observations

The BLK 0 VLBI system was used to generate the VLBI data. This system samples a 1.8 MHz bandpass and allows measurements to be made on sources that are too weak to be observed with the BLK 1 (250 kHz) system which is used for the actual ΔDOR observations. Observations were made in three time-multiplexed channels within the 18-MHz bandpass of the 1.7-GHz receiver. The center frequencies of the channels were 1659.1, 1671.1 and 1676.1 MHz.

The processing of the VLBI data yields a correlated amplitude, CA, which is given by

$$CA = \frac{S\,C\,(\eta_1 \eta_2 A_2 A_2)^{1/2} \times 10^{-26}}{2\,k\,(T_1 T_2)^{1/2}} \qquad (1)$$

where S is the correlated flux density in Janskys, η_1 and η_2 are the aperture efficiencies, A_1 and A_2 are the antenna areas, k is Boltzmann's constant, T_1 and T_2 are the total system temperatures and C is a constant (C = 0.807) which accounts for several effects in the VLBI signal processing. Measurements of the system noise temperature at each antenna and the antenna aperture efficiencies were required in order to calculate the correlated flux densities.

The system temperatures required for converting correlated amplitudes to flux densities were obtained from calibrated strip charts. The efficiency of each antenna is required to get absolute flux from temperature measurements. The efficiency of the 1.7 GHz system at DSS 14 was estimated using radio sources of known flux density in an experiment conducted prior to the VLBI observations.

Observations began in May of 1985 shortly after the 1.7-GHz system on the 64-m antennas became operational. A total of six experiments was performed: Three on the California-Spain baseline and three on the California-Australia baseline. The last observations were conducted in October of 1985. The actual observation time of each experiment was 4 hours. The correlated flux density can have a complicated dependence both on the interferometric hour angle (IHA) and the baseline vector due to spatial structure in the EGRS. The IHA is the difference between the Right Ascension of the perpendicular to the equatorial projection of the baseline vector and the Right Ascension of the source. An attempt was made to observe each source on both baselines and over as wide a range of IHA as possible since it was not known what the IHA would be during ΔDOR observations.

The list of sources to be observed was generated from the existing source catalogue by first selecting all sources that were within 30 deg of the VEGA trajectory (for the period May 1985 to June 1986) and then eliminating those weak sources that were unlikely to be used since they were far from the trajectory or near very strong sources. Because of the criticality of the ΔDOR observations around the region of encounter, all sources in that region were observed regardless of estimated source strength.

III. Results

The total flux density measurements of radio sources with calibrated flux densities provided an estimate for the efficiency of DSS 14 of 0.47. It was assumed that the other 64-m stations had the same value.

Figure 1 shows the distribution on the sky of all of the sources observed and the trajectory of the VEGA spacecraft. A correlated flux density of about 0.4 Janskys (Jy) is required for ΔDOR observations when the antenna system temperature is 40 Kelvin as it is for the 1.7 GHz system. The sources with a correlated flux density of greater than 0.4 Jy are plotted in Fig. 1 with the region within 10 deg of the source marked.

Gaps occur in the coverage along the spacecraft trajectory for several reasons. First, there is a lack of known sources in the direction of the galactic center and anti-center which

causes the gaps around 19 and 6 hours Right Ascension, respectively. A program is currently underway (Ref. 6) to identify suitable navigation sources in these regions. Secondly, observations could not be scheduled for the region from 13 to 16 hours R.A. due to conflicts with other projects. Finally, the sun, which moves on a path very close to the spacecraft path as seen from the Earth, prevented the observation of several sources that would otherwise have been included in the list.

Table 1 lists all of the observed sources along with their correlated flux densities as determined by these measurements. The range of interferometric hour angle for the observations of each source is also listed. Some differences in flux densities were observed between the two baselines and so both are listed in Table 1. Very little variation in flux density with IHA was observed over the limited ranges of IHA observed and thus only the average value is presented in Table 1.

The accuracy of the flux density measurements depends primarily on the accuracy of the system temperature measurements and the measured efficiencies of the antennas. Formal errors in the correlated VLBI amplitudes were generally less than 5%. The error in the efficiency determination was estimated from the uncertainty in the flux density calibration of the radio sources used for calibration and from scatter in repeated measurements. The measured value was 0.47 with an uncertainty of 0.05.

The system noise temperatures (SNTs) were read off of calibrated strip charts. These charts can generally be read with a 1-deg accuracy which corresponds to a 2.5% error. However, drift in temperatures with time made the calibrations of the charts questionable and it was estimated the SNT measurements were no better than 10%.

It is therefore estimated that the statistical error on the correlated flux density measurements is 9% with a systematic error of 11% from the efficiency calibration.

Table 2 lists the positions of all of the sources observed. The positions are given in the J2000 coordinate system and come from the most recent source catalogue, 1986D2.CAT (O. J. Sovers, private communication, 1986).

References

1. Thomas, J. B., "An Analysis of Long Baseline Radio Interferometry," *DSN Technical Report 32-1526*, Vol. *VII*, Jet Propulsion Laboratory, Pasadena, Calif., pp. 37–50, Feb. 15, 1972.

2. Thomas, J. B., "An Analysis of Long Baseline Radio Interferometry, Part II," *DSN Technical Report 32-1526*, Vol. *VIII*, Jet Propulsion Laboratory, Pasadena, Calif., pp. 29–38, April 15, 1972.

3. Thomas, J. B., "An Analysis of Long Baseline Radio Interferometry, Part III, " *DSN Technical Report 32-1526*, Vol. *XVI*, Jet Propulsion Laboratory, Pasadena, Calif., pp. 47–64, June 15, 1973.

4. Melbourne, W. G., and Curkendall, D. W., "Radio Metric Direction Finding: A New Approach to Deep Space Navigation," paper presented at the AAS/AIAA Astrodynamics Specialist Conference, Jackson Hole, Wyoming, Sept. 7–9, 1977; copies are available from the author of this article, K. M. Liewer.

5. Brunn, D. L., Preston, R. A., Wu, C. S., Siegel, H. L., Brown, D. S., Christensen, C. S., and Hilt, D. E., "VLBI Spacecraft Tracking Demonstration: Part 1, Design and Planning," *TDA Progress Report 42-45*, Jet Propulsion Laboratory, Pasadena, Calif., pp. 111–132, Mar.–Apr. 1978.

6. Ulvestad, J. S., and Linfield, R. P., "The Search for Reference Sources for delta-VLBI Navigation of the Galileo Spacecraft," *TDA Progress Report 42-84*, Jet Propulsion Laboratory, Pasadena, Calif., pp. 152–163, Oct.–Dec. 1985.

Table 1. Correlated flux densities at 1.7 GHz

Source	California-Australia		California-Spain	
	I.H.A. Range, hr, min	Correlated Flux Density, Jy	I.H.A. Range, hr, min	Correlated Flux Density, Jy
P 0106+01	1 04 to 1 52	2.9	−13 08 to −12 44	3.7
P 0202+14	−0 12 to 0 36	1.2	−14 12 to −12 16	1.3
CTD 20	−0 14 (1 obs.)	1.6	−14 28 to −13 04	1.6
GC 0235+16	−0 40 to 0 12	0.50	−14 20 to −12 56	0.58
OD 166	−0 36 to 0 12	1.1	−14 04 to −12 48	1.1
GC 0406+12	−0 56 to 1 36	1.1	−14 04 (1 obs.)	0.79
3C 120	−1 16 (1 obs.)	0.25		
P 0420−01	0 48 to 1 28	2.5		
P 0528+134	−0 12 to 2 08	0.61	−10 04 (1 obs.)	0.82
DA 193	0 52 to 1 52	2.1	−10 16 (1 obs.)	2.0
P 0735+17	−0 32 to 0 56	0.58	−11 48 to −9 56	0.67
DW 0742+10	−1 36 to 0 28	1.1	−11 44 to −10 00	2.5
B2 0745+24	0 08 (1 obs.)	0.94	−12 04 to −10 12	0.42
P 0748+126	−0 40 to 0 20	0.58	−11 52 to −11 04	0.37
OJ 425			−11 52 (1 obs.)	1.1
P 0823+033	−1 56 to 0 04	0.51	−12 08 to −11 16	0.90
4C 39.25			−11 28 (1 obs.)	1.5
OL 064.5	−1 56 (1 obs.)	0.79	−12 24 to −11 36	0.54
P 1055+01	−2 04 (1 obs.)	1.1	−12 36 to −12 00	0.70
P 1123+26			−13 20 to −13 00	0.54
P 1127−14			−13 08 (1 obs.)	0.70
P 1222+037			−13 40 to −13 08	1.0
3C 273			−13 40 to −13 08	6.2
P 1519−273	0 40 (1 obs.)	0.63		
DW 1656+05	0 16 (1 obs.)	0.35	−10 48 to −10 12	0.36
P 1657−261	−0 52 (1 obs.)	0.15		
OT-111	−0 56 to 1 20	0.17		
GC 1717+17	0 04 (1 obs.)	0.21	−11 00 (1 obs.)	0.50
NRAO 530	−1 12 to 1 00	1.9	−11 32 (1 obs.)	3.2
P 1741−038	−1 16 to 0 36	1.1	−11 48 to −10 36	1.2
P 1810+10	−0 52 (1 obs.)	0.99	−10 00 to −10 32	0.88
OV-213	−2 16 to −0 −31	<0.06	−12 12 to −11 44	0.92
OV-236	−2 44 to −1 32	3.6		
P 1933−400	−2 48 (1 obs.)	0.22		
OV-198	−2 56 to −0 56	1.2	−12 40 to −11 40	1.1
P 2029+121	−1 36 (1 obs.)	0.37	−14 00 to −12 00	0.59
P 2134+004			−13 28 to −12 44	2.5
P 2145+06			−13 48 to −13 12	0.78
OX 082			−13 40 to −13 08	0.57
OX-192	−2 44 to −2 28	2.0	−12 44 to −12 16	2.4
P 2216−03			−13 16 to −12 52	1.5
3C 446			−13 16 to −13 04	0.87
CTA 102			−13 36 to −13 00	1.0
P 2245−328	−3 28 (1 obs.)	1.3		

Table 2. Positions of observed sources in J2000 coordinates

Source Name	Right Ascension, hr min s	Declination, deg min s	R. A. Error, s	Dec. Error, s
P 0106+01	1 8 38.771114	1 35 0.31866	0.000033	0.00082
P 0202+14	2 4 50.413987	15 14 11.04409	0.000042	0.00088
CTD 20	2 37 52.405765	28 48 8.99121	0.000041	0.00061
GC 0235+16	2 38 38.930211	16 36 59.27431	0.000039	0.00070
OD 166	2 42 29.171033	11 1 0.72725	0.000045	0.00103
GC 0406+12	4 9 22.008811	12 17 39.84798	0.000041	0.00110
P 0420–01	4 23 15.800859	–1 20 33.06536	0.000033	0.00087
3C 120	4 33 11.095640	5 21 15.62095	0.000060	0.00146
P 0528+134	5 30 56.416886	13 31 55.15045	0.000035	0.00075
DA 193	5 55 30.805658	39 48 49.16675	0.000046	0.00055
P 0735+17	7 38 7.393860	17 42 18.99844	0.000037	0.00079
DW 0742+10	7 45 33.059626	10 11 12.69075	0.000032	0.00074
B2 0745+24	7 48 36.109378	24 0 24.10966	0.000046	0.00102
P 0748+126	7 50 52.045858	12 31 4.82675	0.000038	0.00082
OJ 425	8 18 15.999761	42 22 45.41382	0.000049	0.00061
P 0823+033	8 25 50.338476	3 9 24.51846	0.000032	0.00089
4C 39.25	9 27 3.013942	39 2 20.85004	0.000045	0.00060
OL 064.5	10 41 17.162545	6 10 16.92082	0.000035	0.00139
P 1055+01	10 58 29.605239	1 33 58.82181	0.000027	0.00081
P 1123+26	11 25 53.712000	26 10 19.97584	0.000037	0.00080
P 1127–14	11 30 7.052407	–14 49 27.38797	0.000132	0.00201
P 1222+037	12 24 52.421898	3 30 50.29074	0.000038	0.00111
3C 273	12 29 6.699702	2 3 8.59702	0.000001	0.00072
P 1519–273	15 22 37.675997	–27 30 10.78680	0.000113	0.00166
DW 1656+05	16 58 33.447795	5 15 16.43471	0.000408	0.00632
P 1657–261	17 0 53.154298	–26 10 51.72892	0.000061	0.00135
OT-111	17 9 34.345451	–17 28 53.36707	0.000061	0.00139
GC 1717+17	17 19 13.048552	17 45 6.43354	0.000186	0.00329
NRAO 530	17 33 2.705841	–13 4 49.54935	0.000034	0.00101
P 1741–038	17 43 58.856161	–3 50 4.61898	0.000030	0.00087
P 1821+10	18 24 2.855358	10 44 23.77107	0.000078	0.00378
OV-213	19 11 9.652812	–20 6 55.10818	0.000176	0.00252
OV-236	19 24 51.056123	–29 14 30.12252	0.000108	0.00149
P 1933–400	19 37 16.217392	–39 58 1.55016	0.000561	0.00543
OV-198	20 0 57.090601	–17 48 57.67473	0.000060	0.00124
P 2029+121	20 31 54.994196	12 19 41.34210	0.000127	0.00251
P 2134+004	21 36 38.586440	0 41 54.21206	0.000042	0.00097
P 2145+06	21 48 5.458714	6 57 38.60275	0.000029	0.00068
OX 082	21 51 37.875386	5 52 12.95535	0.000052	0.00124
OX-192	21 58 6.281910	–15 1 9.32776	0.000150	0.00227
P 2216–03	22 18 52.037816	–3 35 36.88158	0.000035	0.00095
3C 446	22 25 47.259361	–4 57 1.39173	0.000034	0.00091
CTA 102	22 32 36.408899	11 43 50.90455	0.000035	0.00076
P 2245–328	22 48 38.685744	–32 35 52.18476	0.000147	0.00181

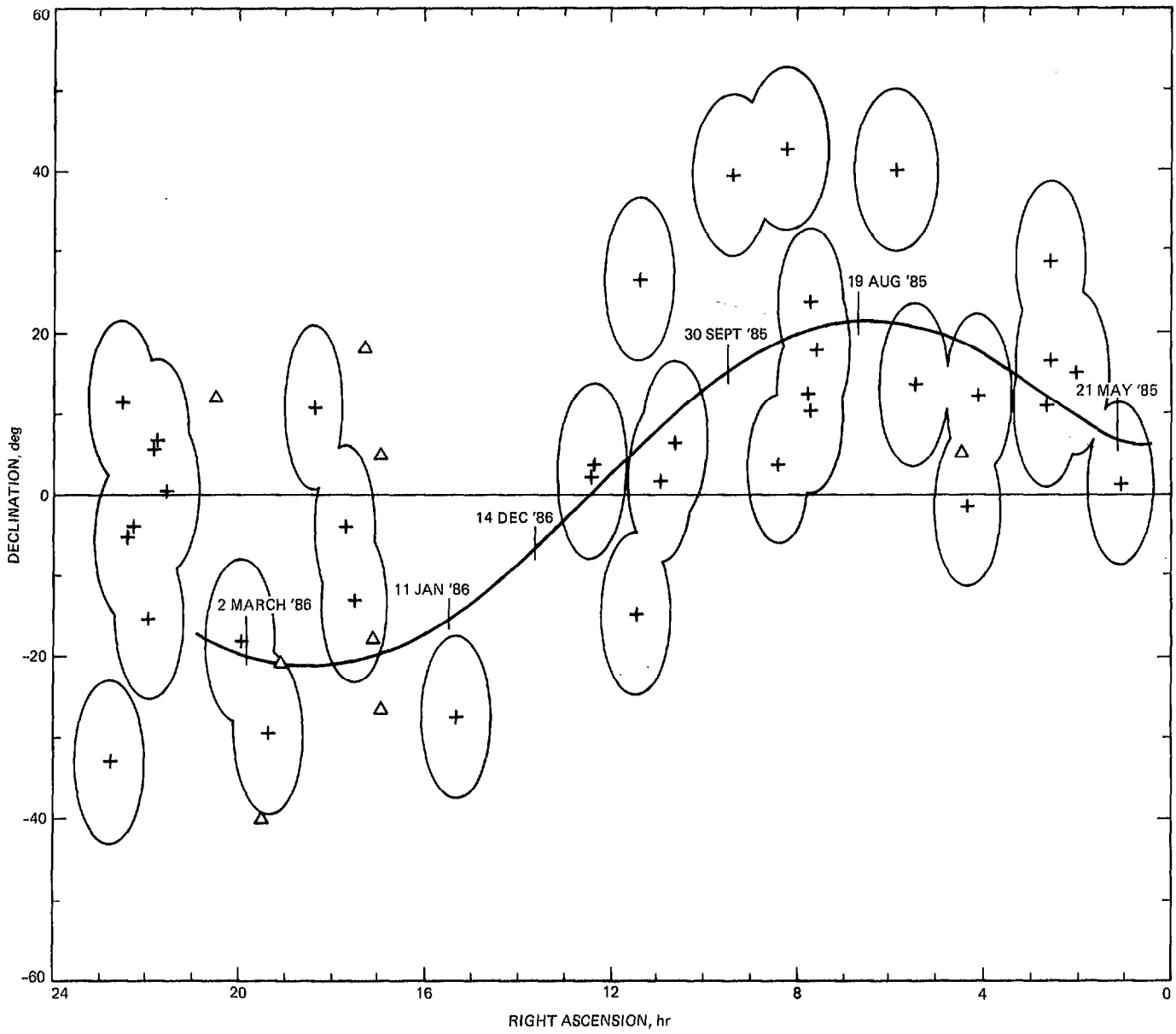

Fig. 1. Distribution of radio sources observed as potential 1.7 GHz VLBI reference sources. Sources with sufficient flux density for use in ΔDOR navigation are plotted as a cross. Those regions within a 10 degree radius of these sources are enclosed by a solid line. Open triangles mark those sources with insufficient flux density. The spacecraft trajectory is shown for the period of May 1985 to March 1986.